Canadian Science Publishing | Canadian Geotechnical Journal

A CPT approach to cable plough performance prediction based upon centrifuge model testing

Journal:	*Canadian Geotechnical Journal*
Manuscript ID	cgj-2020-0366.R1
Manuscript Type:	Article
Date Submitted by the Author:	14-Nov-2020
Complete List of Authors:	Robinson, Scott; University of Dundee, School of Science and Engineering Brown, Michael; University of Dundee, School of Science and Engineering Matsui, Hidetake; Taisei Corporation Brennan, Andrew; University of Dundee, School of Science and Engineering Augarde, Charles; Durham University, Department of Engineering Coombs, William; Durham University, Department of Engineering Cortis, Michael; Wood Group
Keyword:	Cable ploughing, Cone penetration testing, Sand, Centrifuge modelling, Rate effects
Is the invited manuscript for consideration in a Special Issue? :	Not applicable (regular submission)

Date of Original Submission: 30/06/2020

Date of Revised Submission: 14/11/2020

Title: A CPT approach to cable plough performance prediction based upon centrifuge model testing

Author list: Scott Robinson*, Michael John Brown, Hidetake Matsui, Andrew Brennan, Charles Augarde, William Coombs, and Michael Cortis

Author details:

***Corresponding author**

Scott Robinson, MEng PhD MIET FGS GMICE

Lecturer, School of Science and Engineering, University of Dundee, Fulton Building, Dundee, DD1 4HN, UK

ORCID: 0000-0001-6949-8239

Email: s.z.robinson@dundee.ac.uk

Phone: (+44) 01382 386083

Michael Brown, BEng PhD GMICE

Reader, School of Science and Engineering, University of Dundee, Fulton Building, Dundee, DD1 4HN, UK

ORCID: 0000-0001-6770-4836

Email: m.j.z.brown@dundee.ac.uk

Hidetake Matsui, MEng MJSCE MJGS

Research Engineer, Civil Engineering Research Institute, Taisei Corporation, Totsuka, Yokohama, 244-0051, Japan

Email: mtihdt00@pub.taisei.co.jp

Andrew Brennan, MEng PhD GMICE

Senior Lecturer, School of Science and Engineering, University of Dundee, Fulton Building, Dundee, DD1 4HN, UK

ORCID: 0000-0002-8322-0126

Email: a.j.brennan@dundee.ac.uk

Charles Augarde, BSc MSc DPhil CEng FICE

Professor, Department of Engineering, Durham University, Durham, DH1 3LE, UK

ORCID: 0000-0002-5576-7853

Email: charles.augarde@durham.ac.uk

William Coombs, MEng PhD

Associate Professor, Department of Engineering, Durham University, Durham, DH1 3LE, UK

ORCID: 0000-0003-2099-1676

Email: w.m.coombs@durham.ac.uk

Michael Cortis, BEng & Arch (Hons) MSc PhD

Structural Engineer, Wood Group, Aberdeen, AB11 6EQ, UK.

ORCID: 0000-0003-3190-2130

Email: michael.cortis@woodplc.com

Text word count: 8978 (Abstract, main text, acknowledgements and references)

Number of tables: 3 (750 word equivalents)

Number of figures: 11 (2750 word equivalents)

Total word equivalent: 12478

Title: A CPT approach to cable plough performance prediction based upon centrifuge model testing

Authors:

Scott Robinson, Michael John Brown, Hidetake Matsui, Andrew Brennan, Charles Augarde, William Coombs and Michael Cortis

Abstract

Cable ploughing is an important technique for burying and protecting offshore cables. The ability to predict the required tow force and plough performance is essential to allow vessel selection and project programming. Existing tow force models require calibration against full-scale field testing to determine empirical parameters, which may hinder their use. In this study the factors controlling the plough resistance were investigated using a series of dry and saturated 1/50th scale model cable plough tests in sand in a geotechnical centrifuge at 50*g* at a range of target trench depths, sand relative densities and plough velocities. An improved model for predicting cable plough tow force which separates out the key components of resistance and allows tow force prediction without the use of field-derived empirical coefficients is presented. It is demonstrated that the key parameters in this model can be easily determined from in-situ Cone Penetration Testing (CPT), allowing it to be used offshore where site investigation techniques may be more limited compared to onshore locations. The model is validated against the centrifuge cable plough tests, demonstrating it can correctly predict both the static (dry) and rate effect (saturated) tow forces.

Key words: Cable ploughing, CPT, sand, centrifuge modelling, rate effects, offshore

Symbols

a	Stress drop factor
A_{side}	Area of one side of model plough share (below soil)
B	Relevant dimension of object (for boundary effect considerations)
C_d	Dynamic or rate effect coefficient
C_{dn}	Dimensionless dynamic or rate effect coefficient
$C_{dn\psi}$	Dimensionless dynamic or rate effect coefficient incorporating state parameter
C_s	Static coefficient
C_s^*	Modified dimensionless static coefficient
c_v	Coefficient of consolidation
C_w	Plough interface friction ratio
D	Plough depth

1	D_{10}	Representative particle size
2	D_{50}	Mean particle size
3	$D_{v=0}$	Equivalent plough depth at zero velocity
4	D_r	Sand relative density
5	E'_0	One dimensional Young's modulus
6	F	Total plough tow force
7	F_r	CPT friction ratio
8	f_s	CPT sleeve friction
9	F_{static}	Static component of tow force
10	F_w	Self-weight dependent component of tow force
11	$F_{v=0}$	Plough tow force at equivalent of zero velocity or determined during dry testing
12	$F^*_{v=0}$	Plough tow force at equivalent of zero velocity corrected for plough depth changes
13	g	Standard gravitational acceleration
14	K_p	Coefficient of passive earth pressure
15	K_{side}	Coefficient of lateral earth pressure on plough sides
16	N	Scaling factor
17	p'	Mean effective stress
18	p'_{plough}	Mean effective stress at depth relevant to cable ploughing
19	p'_{CPT}	Mean effective stress at depth used for CPT test analysis
20	q_c	CPT cone or tip resistance
21	R_a	Average CPT surface roughness
22	s	Dilation potential
23	S	Distance to boundary/container
24	v	Plough velocity
25	V	Normalised plough velocity
26	w	Plough width
27	W	Plough weight
28	W'	Effective (or buoyant) plough weight
29	δ	Soil-plough interface friction angle
30	δ_{CPT}	Soil-CPT interface friction angle
31	γ	Soil unit weight

1	γ'	Effective soil unit weight
2	η	Methylcellulose dynamic viscosity
3	σ'_{v0}	Initial vertical effective stress
4	φ'_{crit}	Critical friction angle
5	φ'_{max}	Peak friction angle
6	$\Delta\varphi'_{max}$	Change in peak friction angle due to effective stress correction
7	$\varphi'_{max,corr}$	Peak friction angle corrected for effective stresses relevant to cable ploughing
8	ψ	Soil state parameter
9		
10		
11		

12 **Introduction**

13 Cable burial is a key method for the protection of offshore cables from hazards (BERR, 2008) and
14 installation of seabed cables may be undertaken by different means depending on the type of soil
15 encountered (Reece and Grinstead, 1986). One method often used in granular soils is to plough using
16 a specially developed cable plough towed behind a surface vessel (BERR, 2008). The plough consists
17 of a relatively thin vertical cutting tool or share that creates a slot in the ground into which the cable
18 is placed, typically after passing over the rear of the share and exiting at its lower rearward edge
19 (Figure 1). Unlike pipeline ploughing the cable plough does not form a wide v-shaped trench that stays
20 open after ploughing but only supports the soil to allow the cable to exit the share, after which the
21 soil tends to collapse back on top of the cable (ISLES, 2012).
22
23 To allow efficient offshore cable ploughing it is necessary to be able to predict the tow forces required
24 to pull the plough in a certain soil type and the likely progress rates to allow accurate project
25 programming and costing, along with the selection of appropriate equipment (e.g. plough type and
26 vessel). It is also important to ensure that target trench depths are achieved, as these are often
27 contractually specified to ensure sufficient protection of the cable. The tow forces (F) generated
28 during ploughing in sand are associated with interface friction between the cutting and running
29 surfaces of the plough, "static" or passive earth pressure components similar to those encountered in
30 retaining wall design or lateral pile resistance, and velocity (v) dependent soil behaviour associated
31 with the rate of pore pressure equalisation (Lauder *et al.*, 2012; Lauder *et al.*, 2013). Cathie (2001)
32 proposed that these three elements of cable plough tow force resistance in sand could be represented
33 and calculated by Equation 1:

$$F = C_w W + C_s \gamma D^2 + C_d v(C_s \gamma D^2) \quad (1)$$

where C_w is a dimensionless friction coefficient, W is the plough weight, C_s (m) is a non-dimensionless static coefficient, γ is the soil unit weight, D is the depth from the original sand surface to the heel of the plough and C_d (s/m) is a dynamic or rate effect coefficient which is also not dimensionless. To be able to use an approach such as this it is necessary to be able to determine values of C_w, C_s and C_d but this is hindered by the fact that Cathie (2001) does not give any indication of typical values of these parameters or indeed their expected range for cable ploughs. It is, though, instructive to consider experience of the related process of pipeline ploughing. Cathie and Wintgens (2001) provide typical values of similar coefficients for pipeline ploughs which have been back figured from a number of ploughing projects in the field. However, Lauder *et al*. (2013) showed using 1*g* model testing of a single plough configuration that the variation of values proposed for the C_s term, which represents the static plough resistance, was too strongly dependent on relative density compared to model testing experience. Lauder *et al*. (2013) proposed an improved relationship between relative density and C_s with a smaller variation based upon dilation potential and applied to 1*g* testing, which was verified through centrifuge model testing by Robinson *et al*. (2019). Lauder *et al*. (2013) proposed that for pipeline ploughs the C_w term (related to the component of tow force due to self-weight) could simply be represented by the interface properties between the plough and soil material (the interface friction ratio, *tan(δ)*) and that C_w varied to only a limited extent with sand relative density. Based upon 1*g* model testing in loose sand of simple objects representing cable plough shares, Robinson *et al*. (2016*a*, 2017) suggested that, based upon the nature of the shape of a cable plough, it would be more appropriate to include the plough's width as this is a known dimension for each plough, the inclusion of which could help to reduce the dependence of C_s on the specific plough geometry. A method for estimating the 'static' resistance akin to a retaining wall based approach incorporating the plough face dimensions and the passive earth pressure coefficient was suggested as shown in Equation 2. The rate dependency was omitted as this was not investigated by Robinson *et al*. (2017), where dry sand testing was conducted.

$$F_{static} = C_w W + \frac{1}{2} C_s^* K_p^2 \gamma D^2 w \quad (2)$$

where C_s* is a modified dimensionless factor, w is the plough width and K_p is the passive earth pressure coefficient. It is noted that Robinson *et al*. (2017) adopted the term K_p^2 as this is often used to denote the lateral resistance of piles in sand (Barton, 1982), which is a not dissimilar problem. This was to

reflect the contribution of edge effects, where the area of soil ahead of the plough face over which the stress is spread is greater than the area of the plough face itself. This effect would be relatively small for a retaining wall where K_p rather than K_p^2 is adopted. Although adopting Equation 2 reduces the magnitude of the fitting factor C_s (or C_s*), Robinson *et al*. (2017) acknowledged that the factor may still be of a significant magnitude due to the fact that both approaches (Equations 1 and 2) are overly simplistic and fail to represent the separate contributions of the plough leading edge and the large side surface area of a cable plough (Figure 1 and Figure 2). A value of C_s* = 1 would have indicated that all relevant factors had been correctly accounted for, meaning that further factors require consideration. A more complicated theoretically based approach to cable plough force prediction was proposed by Beindorff *et al*. (2012) but the complexity and uncertainty surrounding parameter selection means that this method does not appear to have been applied in a practical setting. As an example, Beindorff *et al*. (2012) uses a large array of parameters (more than 60) to describe the problem, some of which relate to the plough geometry and can be readily obtained, whilst others (such as pore pressures acting on the plough share at a multitude of locations) are heavily dependent on the soil response and are unknown as no guidance on their selection is available. In addition, assumptions on the soil behaviour are made (e.g. the assumption of full passive earth pressure acting on the sides of the share) which have not been experimentally verified. It is clear that a complete plough prediction model must balance theoretical soundness with ease of use for the designer and include guidance on determining each required parameter. This paper therefore aims to investigate the possibility of developing a model for predicting cable plough tow forces based on standard site investigation (SI) tools, namely the Cone Penetration Test (CPT).

The paper presents the result of centrifuge model tests of a series of six cable plough tests undertaken in dry conditions with medium dense and very dense sand, and four further tests undertaken in very dense sand beds saturated with water and Methylcellulose pore fluid solution. The dry tests calibrate the rate independent parameters and the saturated tests simulate a range of plough velocities and allow investigation of cable plough rate effects. Data from CPT tests previously undertaken in-flight (i.e. whilst the centrifuge is spinning) in the same soil material and relative density as that used for the ploughing tests was also analysed to allow correlation with typical offshore SI data. The data from the centrifuge testing is also used to validate the proposed prediction model.

Centrifuge model plough testing

The centrifuge tests were carried out in the Geotechnical Centrifuge Facility at the University of Dundee, using the 3 m radius beam centrifuge (Davies *et al.*, 2001). The centrifuge is capable of applying accelerations of up to 120*g* to model packages of 1 Tonne, although an acceleration of 50*g* was used for this series of tests. Scaling of physical model tests of ploughs has been extensively considered in previous work. The performance of predominantly pipeline ploughs (rather than cable ploughs which are investigated in this paper) was undertaken at 1*g* at a variety of scales to allow a modelling of models approach to verify scaling (Lauder *et al*. 2013 and Lauder and Brown, 2014). This was subsequently validated on the centrifuge at 50*g* by Robinson *et al*. (2019) using specially developed systems to allow pipeline plough testing to occur in-flight. These studies all support the validity of centrifuge and 1*g* small scale model testing (Matsui *et al.*, 2019) to investigate the performance of prototype offshore ploughs. The sand used was a fine silica sand obtained from Congleton in the UK (referred to as HST95), the properties of which are summarised in Table 1.

Model plough

The cable plough tested was a 1/50th scale model of an SMD HD3-300 plough (SMD, 2018) commonly used offshore (Figure 1). The plough share geometry is shown in Figure 2, which includes a plan view (in section) of the leading edge with a 40° internal angle. The model plough has a mass of 0.36 kg (model scale) including instrumentation, corresponding to 45 Tonnes at prototype scale and was fabricated from aluminium to allow the plough mass to be correctly scaled. The cable plough had a maximum possible plough depth of 50 mm (2.5 m at prototype scale). The depth of the plough is controlled by varying the angle of the front skid arms (and trailing arms) with a shallower angle resulting in a deeper target depth. The skid arms were set to the required angle prior to each test using a Vernier protractor (precise to 0.1°). Whilst the plough is set at a target depth, the actual depth achieved is dependent on the test conditions and the balance of forces on the plough share, with higher sand densities and faster velocities (in saturated tests) leading to the plough running at a shallower depth. The plough was designed with a width of 7.5 mm (375 mm at prototype) which is equivalent to 54D_{50} for the soil grains in the sand used. This exceeds the recommendation that the width should be greater than 45D_{50} (for similar cases such as lateral pile testing) by Garnier *et al*. (2007) to ensure that the soil may be considered as a continuum, avoiding grain size effects. Plough instrumentation consisted of a three axis MEMS accelerometer (Analog Devices ADXL377Z) mounted on the top surface of the plough which was designed to measure pitch and roll during testing.

Material, container and actuation system

Testing was undertaken in a specially developed long centrifuge box (with internal dimensions 1500 mm long, 600 mm high and 400 mm wide) which had a bespoke actuation system (Figure 3)

designed to facilitate the large deformation nature of ploughing (described in full by Robinson *et al*., 2019). The box dimensions were shown to be adequate for pipeline ploughing (rather than the cable ploughing considered here) which requires greater distances to box boundaries due primarily to the formation of large surface spoil heaps, and thus indicating that boundary effects would not be an issue. The model cable plough has a width of 7 mm and a horizontal distance to the boundary of 195 mm, which gives a ratio of S/B = 27.8 (where S is the distance to the boundary and B is the cable plough width). This exceeds the recommendation of Garnier *et al.* (2007) that a ratio of S/B = 10 is required to prevent boundary effects. The actuation system consisted of a moving instrumentation platform mounted on linear bearings. The platform actuation was provided by steel reinforced polymer belts on either side of the container, driven by a Parvalux SD12-LWS high torque 220 V DC motor (capacity of 63 Nm at 13 rpm). To make the design as compact as possible, the belts and pulleys were housed within two structural aluminium channels (100 mm x 50 mm x 6 mm) which made up the frame. The system was capable of providing a towing capacity of up to 5 kN, horizontal displacements of up to 800 mm and towing velocities of 28 mm/s (100 m/h). However, due to the enhanced gravity in the centrifuge and the fact that seepage velocity (and hence hydraulic gradient) increase with the scaling factor, N, pore water flow due to shear induced pore pressures around the plough occurs N times faster (Anderson *et al*., 2015; Schofield, 1980; Goodings, 1985). Hence this maximum towing velocity corresponds to a scaled plough velocity of 2 m/h if water were to be used as the pore fluid in saturated tests. Using Hydroxypropyl Methylcellulose (Methocel) as a viscous pore fluid (up to μ = 300 cP) allows this scaled velocity to be increased to 600 m/h. This velocity matches those used in full scale cable ploughing which typically range from 200 - 500 m/h in coarse sands to 50 - 150 m/h in silty sands (ISLES, 2012), with the European Subsea Cables Association indicating that speeds of 200 m/h are typical (KIS-ORCA, 2020). In cable ploughing it is important to differentiate these ploughing velocities from cable laying speeds (where the cable is placed in a pre-cut trench) which can be up to 1000 m/h (BERR, 2008).

A miniature Multicomp SP1-50 draw-wire transducer (DWT) mounted within the frame was used to measure the horizontal displacement of the instrumentation platform. Plough vertical displacement measurements were achieved using a Honeywell MLT004 linear position transducer with a 101 mm range secured to the instrumentation platform, allowing this to be measured throughout the test. The position transducer shaft rested on a 3 mm thick Perspex plate directly above the back face of the plough, which was parallel to the plough base (Figure 1). The force required to tow the plough was measured by a 5 kN Tedea Huntleigh type 616 “S” beam load cell on the towing arm, which the plough was attached to by 2.5 mm diameter stainless steel wire rope (220 mm long). This resulted in typical towing line inclinations of 18 to 25° depending on the set depth of the plough, which the measured

horizontal tow forces were corrected for. Typical towing line inclinations used in the field are nominally of the order of 15° (SMD, 2018), but vary depending on the required cable layback distance and water depths. Further detail of the equipment and its development is given in Robinson *et al*. (2019).

Dry sand bed preparation and testing

For dry sand tests the 150 mm deep sand bed in which the plough is tested was prepared by air pluviation using a slot pluviator (relative densities, D_r, from 41-43% to 83-86% were achieved for the medium dense and very dense beds respectively). The sand bed was pluviated until a height just above the required depth was reached, before the sand surface was levelled with a Perspex scraper. Next the actuator system was placed and bolted into the container and the plough positioned at the starting point and pre-embedded to the target ploughing depth (Table 2). The in-situ characteristics of the sand beds were verified by CPT testing in a separate operation where sand beds were prepared to the same relative density and then tested in flight using a 16 mm diameter CPT mounted on a vertical actuation system (system described in Davidson *et al.* (2018)). The testing programme investigated cable plough behaviour in a range of sand densities, target depths and plough velocities (in the saturated tests) which are summarised in Table 2. The primary results of the testing programme are summarised in Table 3.

Once the centrifuge had reached the required acceleration of 50*g*, a rest period of 5 minutes was allowed to ensure the sensors had fully stabilised. The motor was then activated until a typical horizontal displacement of 750 mm (37.5 m at prototype) had been reached at a speed of 6 mm/s in the dry tests (22 m/h). 50*g* was maintained for a further 5 minutes before the centrifuge was spun down, and the actuator removed from the container. The depth of the plough in this final position relative to the sand surface was measured by hand using a steel rule to record the distance from the top of the container to both the sand surface and the top of the plough, and then accounting for the known depth from the top of the plough to its base. The final pitch and roll of the plough relative to the container was measured using a digital inclinometer with a resolution of 0.1°.

Saturated testing and sample preparation

As mentioned, while the actuator can apply towing speeds of up to 100 m/h, due to the enhanced gravity (*N* times) in the centrifuge the scaled plough velocities would be *N* times lower than would be achieved in a 1*g* test. This is due to the elevated hydraulic gradient in the pore fluid caused by the enhanced gravity, meaning that pore fluid flows (and hence pore pressures dissipate) *N* times faster. To overcome this, a viscous pore fluid with a viscosity of *N* times water (1 cP) could be used (Stewart

et al., 1998). In this case where N = 50, Methylcellulose with a viscosity of 50 cP would allow the 1*g* scaled velocities to be matched. However, to extend the range of scaled plough velocities to that used offshore, Methylcellulose viscosities of up to 326 cP were used to achieve scaled velocities of up to 600 m/h. It is important to differentiate the drainage scaling considered in this paper from (viscous) strain rate effects, which are negligible for sands.

The sand bed was prepared in the same manner as the dry tests, except with the addition of a 35 mm thick layer of gravel below the sand bed which was covered with a layer of geotextile membrane to allow even saturation. The overall height was kept constant resulting in a 115 mm thick sand layer. After the model was loaded onto the centrifuge gondola, and the plough and actuator had been positioned, the model was saturated with Methocel solution. Saturation was carried out via an adjustable valve on the end of the container which was at the position of the gravel layer allowing the flow rate to be controlled such that gradual saturation was achieved over a 24 hour period, minimising air entrapment and sand disturbance. The Methocel solution was brought to 50 mm above the sand surface to ensure that the plough remained fully covered to prevent any changes in the buoyant weight, and the test was run in the same manner as the dry tests at the required towing speed (Table 2). More detail on the Methocel pore fluid preparation and saturation process is given in Robinson *et al*. (2019).

To permit comparison with seabed scans and with results from the companion 3D numerical modelling (Cortis *et al.,* 2017; Cortis *et al.,* 2018), surface scans were taken of the final profile. This was achieved by draining the fluid from the base of the model at 1*g* and scanning the surface with a 3D systems 3D scanner as described in full by Robinson *et al.* (2016*b*) along with verification of its performance and accuracy. This data does not impact on tow force and is not presented here, but is important as it allows comparison with the final surface profiles predicted by the numerical modelling.

Results and discussion

Dry sand testing

In order to separate the “static” and velocity dependent components, both dry and saturated plough testing was undertaken. Typical dry testing results in terms of force and depth variation with distance travelled are shown in Figure 4. This data was derived from a test on a plough pre-embedded to a share depth of 50 mm. In this testing the ploughs were all pre-embedded close to the target plough depth to maximise the length of the steady state data obtained and also because the model ploughs were of fixed geometry whereas a real plough can typically pivot hydraulically close to its mid-point

to aid initial embedment and provide a rapid transition to steady state. Figure 4 shows the plough reaching a steady state associated with a near constant plough depth and relatively constant tow force. The depth and tow force in this region were then averaged for further interpretation. Figure 5 shows the final depth achieved against the target depth, showing that for the dry tests the plough consistently achieved the target depth, with little variation (< 5%) observed.

The data obtained from the dry tests in medium dense and very dense sand at varying depths is shown in Figure 6(a). As there do not appear to be any published C_s values for the model in Equation 1 the value of C_s was varied to give a good match to the centrifuge data with C_s = 4.9 (1.2K_p) in medium dense sand and 6.2 (1.1K_p) in very dense sand. The values of C_s are given relative to K_p using peak friction angles determined by:

$$\varphi'_{max} = 29 + 18\left(\frac{D_r}{100}\right) \quad (3)$$

based on triaxial testing of the HST95 sand used here conducted at stresses relevant to ploughing (p'_0 = 20 to 60 kPa). This stress range is slightly higher than would be expected for fully drained cable ploughing, which is to account for the fact that the dataset is also used for high velocity saturated tests where negative pore pressure changes (and increased effective stresses) occur. The relationship is based upon the approach proposed by Bolton (1986). For a model based on Equation 1, the variable C_s is required as an empirical parameter to cover a range of otherwise unquantified factors. For the alternative model presented in Equation 2, where passive pressure and edge effects have been removed from C_s to leave the factor C_s^*, the data shows that values of C_s^* = 2.5 for medium dense sand and C_s^* = 3.3 for very dense sand were found (Figure 6(b)). Robinson *et al*. (2017) noted that a value of C_s* of 1 would indicate that all factors that influence tow force had been accounted for outside of the empirical coefficient. Hence these values of C_s* suggest an improvement compared to Equation 1, but that a further significant component of resistance remains unaccounted for explicitly.

In an attempt to improve upon Equation 1 and 2 it was decided to modify Equation 2 and separate out the contributions from the front face or plough leading edge and the plough sides as suggested by Robinson *et al*. (2017) leading to Equation 4. This was based on insights from testing of simple 1*g* plough analogues which highlighted the potential for the separation of plough face and side resistances.

$$F = C_w W + \tfrac{1}{2} 3 K_p \gamma D^2 w + 2\left[\tfrac{1}{2} K_{side} \gamma D A_{side} \tan(\delta)\right] \quad (4)$$

where K_{side} is the lateral earth pressure experienced on the plough sides after the sand has passed the leading edge of the plough, A_{side} is the submerged (below soil) surface area of one side of the plough that varies with depth and δ is the sand-aluminium interface friction angle.

As Equation 4 aims to remove the need for the empirical coefficient, C_s, it is necessary to ensure that the model correctly captures the influence of varying soil density on the static tow force, which was previously combined into this parameter. This is included via the passive earth pressure coefficient K_p, which increases with peak friction angle that is in turn dependent on the relative density. As previously noted, two correlations between lateral resistance (incorporating edge effects) and K_p were proposed by Barton (1982) and Broms (1964), which suggested that the lateral resistance of piles varied with K_p^2 and $3K_p$ respectively. Robinson *et al*. (2017) suggested that the use of K_p^2 may be suitable, however, trials of this method using the centrifuge cable plough data indicated that this led to the prediction of a greater variation in tow force with density than that measured. Instead, using $3K_p$ as proposed by Broms (1964) correctly captured the magnitude of the tow force sensitivity to relative density. Hence, Equation 4 uses this approach rather than that previously suggested by Robinson *et al.* (2017). Possible reasons for this include the fact that Robinson *et al*. (2017) used 1*g* model testing, which may overestimate dilation compared to full scale or centrifuge tests due to the low effective stress at 1*g*.

A key parameter in Equation 4 which requires identification is the lateral earth pressure coefficient on the plough sides, K_{side}. A literature review identified that there is currently no guidance on this parameter, and assumptions are often made regarding its value. For example, Beindorff *et al*. (2012) suggested that K_p (based on φ'_{crit}) may be used, but there is no experimental verification of this. There are existing approaches for identifying K_{side} for other geotechnical problems, such as piles, and Lehane *et al.* (2005) suggested (to allow estimation of pile shaft capacity) that this could be done by CPT testing using the measured sleeve friction, the steel-sand interface friction ratio and the expected initial vertical effective stress at any given depth. Hence K_{side} can be estimated using Equation 5:

$$K_{side} = \frac{\sigma'_h}{\sigma'_v} = \frac{f_s}{\sigma'_v \tan(\delta_{cpt})} \quad (5)$$

where f_s is the CPT sleeve friction and δ_{cpt} is the CPT-soil interface friction angle. Sleeve friction measurements in the field can be variable, hence Lehane *et al.* (2005) suggested that this may alternatively be estimated from the cone resistance, q_c, by using an assumed typical friction ratio, F_r, of 0.01 for sands such that Equation 5 may be rewritten as:

$$K_{side} = \frac{F_r q_c}{\sigma'_v \tan(\delta_{cpt})} \quad where\ F_r = 0.01\ for\ sands \tag{6}$$

It is simplistically assumed that the passage of the CPT through the soil is similar to the leading edge of the plough and that a similar, even if slightly different in magnitude, stress regime may be experienced, namely high stress in advance of the cone with significant stress drop on moving from the face of the cone (or plough leading edge) to the shoulder and onto the sleeve (or plough side walls). Hence 16 mm model CPT tests conducted in flight at 50*g* in sand beds prepared with the same properties as those used in the plough tests were analysed to investigate the likely values of K_{side} for cable ploughing in HST95 sand. The centrifuge CPT tests had a minimum distance to a boundary of 250 mm (S/B = 15.6), which indicates boundary effects should not occur as Garnier *et al.* (2007) state that a ratio of S/B = 10 is sufficient to prevent this. Figure 7 show the results of CPT tests conducted at relative densities of 53% and 84%. Both tests show the expected trend of increasing tip and sleeve resistance with depth, along with both of these parameters increasing with relative density. Analysis of CPT tests is problematic in the first few metres near-surface (due to the transition to a steady state mechanism with depth), but derived friction ratios were found to tend towards F_r = 0.015 in medium dense sand and F_r = 0.007 in very dense sand at depth. These compare well with the value of 0.01 adopted by Lehane *et al*. (2005), where variation with density was not included. Figure 8 shows the calculated lateral stress coefficients, K_{side}, using Equation 6 based on the measured friction ratios.

A key variable in this analysis is the value of δ_{cpt}, for which Lehane *et al*. (2005) adopted a value of 18° due to the expectation that the CPT cone would be rapidly worn and smoothed by repeated use in sand. Using an accurate value for δ_{cpt} is essential to ensure correct estimation of K_{side}, especially when using a model CPT cone where the wear may be far less than in the field. Dejong *et al*. (2001) considered this issue in detail and found that for a new cone with an average roughness, R_a, of 0.5 ± 0.25 µm (to ASTM standard), the interface friction angle, δ_{cpt}, was 24° in sand which is also in keeping with the findings of Uesugi and Kishida (1986). Analysis of actual CPT cones identified that new cones had an average surface roughness of 0.28 to 2.08 µm and that cones that had been used in the field had an average roughness of 0.18 to 6.85 µm suggesting that cone roughness does not necessarily

reduce with use, but does become more variable. The roughness of the model CPT cone used in the tests was measured using a Taylor Hobson Surtronic Duo, and was found to have an average roughness of 0.6 µm (within ASTM standard). Hence in the analysis presented herein, δ_{cpt} = 24° was adopted as recommended by Dejong *et al*. (2001). In the field, where recent measurements of δ_{cpt} for the specific CPT in question have been obtained from interface tests, alternatively these values may be used instead.

Lehane *et al*. (2005) suggested that a stress drop factor (the ratio of lateral stress to vertical tip stress), a, of 0.03 could be used. This value is based on an assumed value of F_r = 0.01 and δ = 18° ($tan(\delta)$ = 0.33). For the value of δ = 24° used here and the values of F_r = 0.015 and 0.007 from the CPT testing, the stress drop factor was found to range from a = 0.034 to 0.016 for medium dense and very dense sand, respectively. This suggests that the stress drop factor may have some density dependence not mentioned by Lehane *et al*. (2005). This stress dependence would be in keeping with the CPT soil identification chart proposed by Robertson *et al*. (1986) which suggests F_r (and hence the stress drop factor, a) reduces with increasing relative density. Previous density dependency of the stress drop factor was also noted by Al-Baghdadi (2018) when predicting screw pile behaviour from CPT testing.

The values of K_{side} = 1.6 to 1.7 found from the CPT testing correspond to 0.49K_p and 0.52K_p (K_p based on φ'_{crit}) respectively, suggesting that the assumption used by Beindorff *et al*. (2012) for cable ploughs of $K_{side} = K_p$ may be incorrect. K_{side} also appears to be relatively independent of density when compared to F_r and a. Again, this would be in keeping with Robertson *et al*. (1986), as $K_{side} \propto F_r q_c$. Robertson *et al*. (1986) showed that with increasing relative density, F_r reduces and q_c increases, explaining the apparent density independence.

Given that K_{side} could be estimated from CPT testing using either measured sleeve friction or from q_c using an assumed friction ratio, this means that the component of resistance from interface friction on the plough sides in Equation 4 can be calculated. This raises the prospect of a CPT based method for calculating the overall plough resistance. However, to achieve this, it is necessary to consider how the plough face resistance can be predicted using the same CPT information. Equation 4 sets out the proposed relationship between the soil properties and face resistance, namely that face resistance is proportional to 3K_p. The question of how the value of K_p is selected from CPT tests for this specific application still remains. Analysis up to this point uses known peak friction angles for the HST95 sand used which were based on element testing at the corresponding relative density.

K_p is related to the internal friction angle, φ', by Equation 7, and the peak friction angle may in turn be derived from the CPT tip resistance, q_c, using an approach such as that proposed by Knappett and Craig (2019) shown in Equation 8 (for silica sands). This approach assumes that the CPT test is drained,

and is a standard method for determining φ'_{max} from CPT data. Using this approach, φ'_{max} was calculated from the CPT data shown in Figure 7, taken at a prototype depth of 5 m in order to avoid the issues interpreting CPT data near-surface. This yielded values of φ'_{max} = 35.6° and 40.5° for the medium dense and very dense HST95 samples respectively.

$$K_p = \frac{1+sin(\varphi')}{1-sin(\varphi')} \quad (7)$$

$$\varphi'_{max} = 6.6 + 11log\left(\frac{q_c}{\sigma'^{0.5}_{v0}}\right) \quad (8)$$

where σ'_{v0} is the initial vertical effective stress at the depth at which q_c is selected.

Figure 9(a) shows the variation of the proposed tow force prediction model with depth (Equation 4) using the values of K_{side} and φ'_{max} derived using the CPT based approach. Note that unlike Figures 4 and 5 where curves were fitted to fit data, these curves have been derived independently of the measured tow forces (true predictions). Compared with the measured tow forces at each relative density, in both cases it can be seen that the model generally underpredicts the tow force, particularly in very dense HST95. As this underprediction correlates with relative density, this suggests that either the model is insufficiently emphasising the role of dilation or the CPT - φ'_{max} correlation is an underestimation. As the ploughing occurs near-surface in soil at low effective stress, and the CPT measurements had to be taken from a depth of 5 m, this suggests the CPT measurement at 5 m was at too great an effective stress to capture the low-stress dilatancy of the soil or that any effective stress correction in equation 8 is not sensitive enough at these shallow depths. Correcting for this is therefore necessary to improve the fit to the data in Figure 9(a).

The dilation angle and its variation with relative density and mean effective stress can be represented by Equation 9 for sands (Bolton, 1986). Taking the finite difference of Equation 9 allows the change in dilation angle between the two points of differing log initial mean effective stress, *ln(p')*, at a given relative density to be approximated (Equation 10). By selecting a depth relevant to ploughing of 1.5 m (2/3 of the average plough depth used in the test programme which is the resultant force location), Equation 10 and 11 can be used to correct the values of φ'_{max} derived from the CPT testing for the lower effective stress conditions near-surface, yielding stress corrected values of φ'_{max} = 37.3° and

43.6° for medium dense and very dense HST95 sand respectively, compared to the original values of 35.6° and 40.5°.

$$\varphi'_{max} = 3D_r\left[10 - ln\left(p'\right)\right] - 3 \quad (9)$$

$$\Delta\varphi'_{max} = 3D_r\left[ln\left(p'_{cpt}\right) - ln\left(p'_{plough}\right)\right] \quad (10)$$

$$\varphi'_{max,corr} = \varphi'_{max} + \Delta\varphi'_{max} \quad (11)$$

Figure 9(b) shows the tow force prediction using Equation 4 with the stress corrected CPT friction angles, indicating that the proposed model now fits the measured centrifuge model plough testing data well. This suggests that the CPT based approach described could provide a useful way to predict overall plough tow forces where the only available characterisation is in-situ CPT testing. The model removes the need to use empirical factors to predict the plough resistance, which would have required characterisation for each plough design before use, and relates the overall tow force to the main specific components that contribute to the plough resistance. Having established that CPT can be linked to low effective stress regimes and can be used to give reasonable predictions in place of the previous empirical C_s coefficients, it is recommended to further validate this on a wider range of plough geometries and soil conditions.

Saturated sand testing

Up to this point, the analysis has considered only dry testing which does not include rate effects on the plough resistance. These occur due to the fact that as the plough velocity increases, there is less time for negative pore pressures (caused by dilation as soil is sheared by the plough) to dissipate, leading to an increase in the effective stress in the soil around the plough (Lauder *et al.*, 2012). Cathie (2001) proposed a model for accounting for rate effects on the cable plough tow force (Equation 1) but as previously noted, the rate effect coefficient, C_d, is not dimensionless and varies depending on the soil state and properties. Lauder *et al*. (2013) proposed a rate effect model for pipeline ploughs which has the advantage of including a dimensionless parameter, C_{dn}, and accounts for the soil state and properties via the dilation potential, *s*, (Palmer, 1999) and the coefficient of consolidation, c_v (Equation 12). This builds on the concept of the normalised velocity, $V = vd/c_v$, which is used in many applications where drainage effects are a consideration (e.g. Finnie and Randolph, 1994; Colreavy *et*

al., 2016). The normalised velocity is also extensively used in pipeline ploughing studies (Lauder *et al.*, 2012; Lauder *et al.*, 2013; Robinson *et al.*, 2019).

$$F = \left(C_w W' + C_s \gamma' D^3\right)\left(1 + C_{dn}\frac{svD}{c_v}\right) \quad (12)$$

This equation may be rewritten to be suitable for cable ploughing as shown in Equation 13, the key terms of which can be found using the equations set out earlier. This accounts for rate effects in a similar manner to Equation 12, but with the dilation potential, *s*, replaced with the state parameter, ψ. The reason for this is that the aim of this paper is to develop a CPT based approach, and the state parameter can be more easily obtained from CPT testing (e.g. Shuttle and Jefferies, 2016) than the dilation potential. Hence the dynamic coefficient is renamed $C_{dn\psi}$, which nevertheless remains dimensionless. As the conventional definition of ψ is that dilatant soils have a negative state parameter, a negative sign is also included in Equation 13.

$$F = \left(C_w W' + \tfrac{1}{2} 3 K_p \gamma' D^2 w + 2\left[\tfrac{1}{2} k_{side} \gamma' D A_{side} \tan(\delta)\right]\right)\left(1 + C_{dn\psi}\frac{-\psi vD}{c_v}\right) \quad (13)$$

Figure 10(a) shows the variation of tow force with plough velocity for the saturated cable plough tests in very dense sand which were stable (defined as final depth achieving at least 90% of target depth). The increase in tow force with velocity can be clearly seen, but another important point to note is that in contrast to the dry testing where the plough consistently achieved the target depths, in the saturated tests the cable plough's final depth (Table 3) varied with its velocity (up to 10% reduction in depth at v = 318 m/h). Figure 10(b) shows the change in the normalised depth (the final plough depth divided by the final depth of the reference test at zero velocity (conducted in dry conditions where rate effects do not occur)) with velocity for the saturated tests which, whilst being less significant than that found in pipeline ploughing (over the velocity range tested), still needs to be accounted for. This is because tow force is highly sensitive to depth changes, varying with D^2. Hence it is important to use the actual final depths achieved in Equation 13 rather than target depth. Similarly, when normalising tow force (Figure 11), the reference force, $F^*_{v=0}$, used to normalise the y-axis should correspond to this actual final depth rather than the target depth. As described by Robinson *et al.* (2019), this means

that $F^*_{v=0}$ should be the zero velocity (reference) force that would have been expected if the reference plough test had achieved exactly the same final depth as the dynamic test (in order to account for the fact that the final depth would have varied between them).

Before $C_{dn\psi}$ can be determined from the test data, a further consideration is the method by which state parameter, ψ can be estimated from the CPT data. A number of approaches are available such as Been *et al.* (1987) or Sadrekarimi (2016), but these require information such as empirical coefficients which in turn are related to critical state parameters to allow ψ to be found; information which may not necessarily be available from CPT base site investigation alone. Alternatively, Been and Jefferies (1985) showed a correlation between ψ and φ'_{max}, but no equation was fitted to this data to allow the correlation to be used. The data from Been and Jefferies (1985) was sampled and for ease of use, Equation 14 is proposed to allow this correlation to be used to find ψ from φ'_{max} based on CPT testing. This correlation is valid for the range of φ'_{max} investigated by Been and Jefferies (1985) (φ'_{max} from 30° to 48°). An additional advantage of this approach is that the $\varphi'_{max,corr}$ corrected for near-surface dilatancy (Equation 10) may also be used here. Values of state parameter obtained using Equation 14 compared well with known state parameters for HST95 sand from triaxial element testing at the same relative density. The coefficient of consolidation, c_v, may also be determined (although a lab testing approach was used here, similar to Robinson *et al.*, 2019) from CPT dissipation tests (e.g. Chow *et al.*, 2014; Colreavy *et al.*, 2016), in keeping with the aim of creating a fully CPT based approach.

$$\psi = 23.2\varphi'^{-0.9}_{max,corr} - 1 \quad (14)$$

Figure 11 shows the rate effect on the plough tow force in the stable saturated tests against the normalised velocity based on the state parameter, with the rate effect increasing with the normalised velocity. The relationship is relatively linear for the range of velocities considered (up to v = 318 m/h), which is similar to the relationship found for pipeline ploughs by Lauder *et al*. (2013). The gradient of this line represents the dimensionless rate effect coefficient $C_{dn\psi}$, which for the model cable plough was found to be 0.78. It is important to note the sign of the normalisation on the x-axis, which is due to the adoption of the conventional definition of ψ, where dilatant soils have a negative state parameter. Tests conducted at higher velocities will be considered in future publications due to the fact that these tests demonstrated varying degrees of plough instability (as can be observed in the field), and this instability requires further aspects to be considered when modelling plough rate

effects. It is also important to note that the rate effect correlations determined here are valid for sands, and that additional care should be taken when considering sands with a significant silt content which experience suggests may be an area where further research is required. This is due to the potential for the silt content to influence the state parameter and soil permeability, both of which are important when predicting rate effects. Nevertheless, the CPT based approach for the prediction of static tow forces (both plough face and sides), combined with the rate effect correlation with the state parameter, allows Equation 13 to be used. This allows overall tow forces to be predicted solely from CPT testing, and avoids the need to use empirical coefficients often required in current methods that are not currently available in the public domain.

Summary and conclusions

To investigate the behaviour of offshore cable ploughs, 50*g* centrifuge testing of a 1/50th scale model cable plough was conducted at the University of Dundee's 3m radius geotechnical centrifuge facility using specially developed large displacement plough testing equipment. The testing investigated a range of variables including plough depth and sand relative density, as well as both dry and saturated conditions to allow rate effect behaviour to be considered. Plough velocities of up to 600 m/h were tested, covering the typical range of velocities used in the field.

A model has been presented which separates the two key components of plough resistance, namely the passive 'face' resistance on the leading edge and the interface friction on the plough sides. The model avoids the use of empirical coefficients for these by relating the face resistance to the passive earth pressure coefficient, K_p, and the side resistance to the lateral earth pressure, K_{side}, as well as accounting for the share width. The rate effect response of the plough was also incorporated using a normalised velocity linked to the soil state parameter, ψ. It was shown that these parameters can be predicted using only CPT testing, allowing the model to be used in offshore conditions where material characterisation may be more limited. Analysis of centrifuge (50*g*) CPT tests with a 16 mm cone in model sand beds with the same relative densities as for the ploughing tests were used to demonstrate the derivation of these key parameters, and to allow the CPT based approach to be validated against the centrifuge cable plough testing results. The model correctly captured the cable plough tow force behaviour, suggesting it may provide a useful tool to more easily predict cable plough tow forces on site and avoid the need for empirical coefficients calibrated to each specific plough design.

Data Access Statement

The data presented in this paper is available online via the University of Dundee's institutional repository and may be accessed at: https://doi.org/10.15132/10000161

Acknowledgements

The model seabed ploughing described in this paper was undertaken for the EPSRC funded project Seabed ploughing: modelling for infrastructure installation (EP/M000362/1 and EP/M000397/1). The 3D surface scanning technique and centrifuge ploughing actuation systems were developed as part of the Scottish Marine and Renewables Test (SMART) Centre at the University of Dundee, funded by the European Regional Development Fund (ERDF).

References

Al-Baghdadi, T. (2018) Screw piles as offshore foundations: Numerical and physical modelling. *PhD Thesis*, University of Dundee, Dundee, UK.

Anderson, C., Sivakumar, V. and Black, J.A. (2015) Measurement of permeability using a bench-top centrifuge. *Géotechnique*, **65**(1): 12-22.

Barton, Y.O. (1982) Laterally Loaded Model Piles in Sand: Centrifuge Tests and Finite Element Analyses. *PhD Thesis*, University of Cambridge, UK.

Beindorff, R., Miedema, S.A. and Van Baalen, L.R. (2012) Calculations on forces and velocities of a submarine narrow trench plough in sandy soil. *Terra et Aqua*, International Association of Dredging Companies, **126:** 13-24.

BERR (2008) *Review of Cabling Techniques and Environmental Effects Applicable to the Offshore Wind Farm Industry*, Department for Business, Enterprise and Regulatory Reform, Her Majesty's Government, London, UK. Available at http://randd.defra.gov.uk/Document.aspx?Document=ME1108_7409_FRP.pdf. Accessed 01/02/2020.

Bolton, M.D. (1986) The strength and dilatancy of sands. *Géotechnique*, **36**(1): 65-78.

Broms, B.B. (1964) Lateral resistance of piles in cohesionless soil. *Journal of Soil Mechanics and Foundation Division*, ASCE. **90**(SM3): 123-156.

Brown, M.J., Bransby, M.F., Knappett, J.A., Tovey, S. Lauder, K. and Pyrah, J. (2015) The effect of buried fibres on offshore pipeline plough performance. *Ocean Engineering*, **108**: 760-768. DOI: 10.1016/j.oceaneng.2015.08.022.

Cathie, D. (2001) Advances in burial assessment and performance prediction. *International Cable Protection Committee (ICPC) Plenary Meeting*, Tokyo, Japan. May 2001.

Cathie, D.N. and Wintgens, J-F. (2001) Pipeline trenching using plows: performance and geotechnical hazards. *Proceedings of the 33rd Annual Offshore Technology conference (OTC)*, Houston, USA, 1-14.

Chow, S.H., O'Loughlin, C.D. and Randolph, M.F. (2014) Soil strength estimation and pore pressure dissipation for free-fall piezocone in soft clay. *Géotechnique*, **64**(10): 817-827.

Colreavy, C., O'Loughlin, C.D. and Randolph, M.F. (2016) Estimating consolidation parameters from field piezoball tests. *Géotechnique*, **66**(4): 333-343.

Cortis, M., Coombs, W.M., Augarde, C.E., Robinson, S., Brown, M.J. and Brennan, A.J. (2017) Modelling seabed ploughing using the material point method. *Procedia Engineering*, **175**: 1-7. DOI: 10.1016/j.proeng.2017.01.002.

Cortis, M., Coombs, W.M., Augarde, C.E., Brown, M.J., Brennan, A.J. and Robinson, S. (2018) Imposition of essential boundary conditions in the material point method. *International Journal for Numerical Methods in Engineering*, **113**(1):130-152. DOI: 10.1002/nme.5606.

Davidson, C., Al-Baghdadi, T., Brown, M.J., Knappett, J., Brennan, A., Augarde, C.E., Wang, L., Coombs, W.M., Richards, D., Blake, A. and Ball, J. (2018) Centrifuge modelling of screw piles for offshore wind energy foundations. *Proceedings of the 9th International Conference on Physical Modelling in Geotechnics (ICPMG 2018)*, 17-20 July 2018, London, UK. CRC Press, 695-700. DOI: 10.1201/9780429438646.

Davies M.C.R., Newson T.A. and Bransby M.F. (2001) Geotechnical centrifuge modelling at the University of Dundee. *Proceedings of the International Symposium on Geotechnical Centrifuge Modelling and Networking*, Hong Kong. CRC Press, 15-16.

Dejong, J.T., Frost, J.D. and Cargill, P.E. (2001) Effect of surface texturing on CPT friction sleeve measurements. *Journal of Geotechnical and Geoenvironmental Engineering*, ASCE, **127**(2): 158-168.

Finnie, I.M.S. and Randolph, M.F. (1994) Punch-through and liquefaction induced failure of shallow foundations on calcareous sediments. *Proceedings of the International Conference on Behaviour of Offshore Structures*, Boston, Massachusetts, USA, 217-230.

Garnier, J., Gaudin, C., Springman, S.M., Culligan, P.J., Goodings, D., Konig, D., Kutter, B., Phillips, R., Randolph, M.F. and Thorel, L. (2007) Catalogue of scaling laws and similitude questions in geotechnical centrifuge modelling. *International Journal of Physical Modelling in Geotechnics*, **7**(3): 1-23.

Goodings, D.J. (1985) Relationships for modelling water effects in geotechnical centrifuge models. *Proceedings of a Symposium on the Application of Centrifuge Modelling to Geotechnical Design*, Manchester, 16-18 April 1984. Balkema, Rotterdam, The Netherlands.

ISLES (2012) *Irish-Scottish Links on Energy Study (ISLES): Construction and Deployment Report*. Isles Project. Available at http://www.islesproject.eu/wp-content/uploads/2014/09/8.0-Construction-and-Deployment.pdf. Accessed 10/02/2020.

KIS-ORCA (2020) *Kingfisher Information Service - Offshore Renewable and Cables Awareness: Guidance on Cable Burial*. European Subsea Cables Association (ESCA), Guisborough, North Yorkshire, UK. Available at https://kis-orca.eu/subsea-cables/cable-burial/. Accessed 05/02/2020.

Knappett, J.A. and Craig, R.F. (2019) *Craig's Soil Mechanics (9th Edition)*, CRC Press, Abingdon, UK.

Lauder K.D. (2011) The performance of pipeline ploughs. *PhD Thesis*, University of Dundee, UK.

Lauder, K. and Brown, M.J. (2014) Scaling effects in the 1g modelling of offshore pipeline ploughs. *Proceedings of the 8th International Conference on Physical Modelling in Geotechnics (ICPMG 2014)*, Perth, Western Australia. CRC Press, 377-383.

Lauder, K., Brown, M.J., Bransby, M.F. and Gooding, S. (2012) The variation of tow force with velocity during offshore ploughing in granular materials. *Canadian Geotechnical Journal*, **49**(11): 1244-1255. DOI: 10.1139/t2012-086.

Lauder, K., Brown, M.J., Bransby, M.F. and Boyes, S. (2013) The influence of incorporating a forecutter on the performance of offshore pipeline ploughs. *Applied Ocean Research*, **39**: 121-130. DOI: 10.1016/j.apor.2012.11.001.

Lehane, B.M., Schneider, J. and Xu, X. (2005) The UWA-05 method for prediction of axial capacity of driven piles in sand. *Proceedings of the 1st International Symposium on Frontiers in Offshore Geotechnics (ISFOG 2005)*, Perth, Australia, 683-689.

Lunne, T., Robertson, P.K. and Powell, J.J.M. (1997) *Cone Penetration Testing in Geotechnical Practice*. CRC Press, Abingdon, UK.

Matsui, H., Robinson, S., Brown, M.J., Brennan, A.J. Cortis, M., Coombs, W.M., & Augarde, C.E. (2019) Investigation into the effect of plough share leading geometry angle on cable plough performance. *Proceedings of the 16th Asian Regional Conference on Soil Mechanics and Geotechnical Engineering (16 ARC)*, Taipei, Taiwan, 14-18 October 2019.

Palmer, A.C. (1999) Speed effects in cutting and ploughing. *Géotechnique*, **49**(3): 285-294.

Reece, A.R. and Grinsted, T.W. (1986) Soil mechanics of submarine ploughs. *Proceedings of the Eighteenth Annual Offshore Technology Conference, Houston, Texas*, USA, 453-461.

Robertson, P.K., Campanella, R.G., Gillespie, D. and Greig, J. (1986) Use of piezometer cone data. *Proceedings of the ASCE Specialty Conference In Situ 1986: Use of In Situ Tests in Geotechnical Engineering*, Blacksburg, ASCE, 1263-1280.

Robinson, S., Brown, M.J., Brennan, A.J., Cortis, M., Augarde, C.E. and Coombs, W.M. (2016*a)* Improving seabed cable plough performance for offshore renewable energy. *Proceedings of the 2nd International Conference on Renewable Energies Offshore (Renew 2016*) Lisbon, Portugal. Taylor & Francis, London, 413-419.

Robinson, S., Brown, M.J., Brennan, A.J., Cortis, M., Augarde, C.E. and Coombs, W.M. (2016*b*) Development of low cost 3D soil surface scanning for physical modelling. *Proceedings of the 3rd European Conference on Physical Modelling in Geotechnics (Eurofuge 2016)*, Nantes, France, 1-3 June 2016. IFFSTAR, Nantes, 159-164.

Robinson S., Brown M.J., Brennan A.J., Cortis M., Augarde C.E. and Coombs W.M. (2017) Improvement of seabed cable plough tow force prediction models. *Proceeding of the 8th International Conference on Offshore Site Investigation & Geotechnics (SUT OSIG), London, UK*. Society for Underwater Technology (SUT), UK, 914-921.

Robinson, S., Brown, M.J., Brennan, A.J., Cortis, M., Augarde, C.E. and Coombs, W.M. (2019) Centrifuge testing to verify scaling of offshore pipeline ploughs. *International Journal of Physical Modelling in Geotechnics*, **19**(6): 305-317. DOI: 10.1680/jphmg.17.00075.

Schofield, A.N. (1980) Cambridge geotechnical centrifuge operations. *Géotechnique*, **30**(3): 227-268.

SMD (2018) *HD3-300 Heavy Duty Plough Specifications*, Soil Machine Dynamics Ltd, Newcastle-upon-Tyne, UK. Available at https://www.smd.co.uk/wp-content/uploads/2017/01/HD3-300.pdf_0.pdf. Accessed 16/01/2019.

Uesugi, M. and Kishida, H. (1986) Frictional resistance at yield between dry sand and mild steel. *Soils and Foundations*, **26**(4): 139-149.

Table Caption List

Table 1 - Properties of HST95 sand used in the centrifuge tests.

Table 2 - Summary of centrifuge testing programme using a 1/50th scale model cable plough in HST 95 sand.

Table 3 - Summary of primary results from the centrifuge testing programme using a 1/50th scale model cable plough in HST 95 sand.

Figure Caption List

Figure 1 - Image showing the 1/50th scale aluminium model cable plough instrumented with MEMS accelerometer for pitch and roll sensing.

Figure 2 - (a) Side elevation of 1/50th scale model cable plough in ploughing configuration showing key share dimensions, (b) incorporating plan view (in section) of tip geometry (dimensions in mm at model scale).

Figure 3 - Schematic showing a cross section of the large displacement centrifuge ploughing actuator and model.

Figure 4 - Variation of pre-embedded model cable plough tow force and depth with displacement from a centrifuge test in very dense dry HST95 sand (D_r = 86 %) with a target depth of 50 mm (at model scale).

Figure 5 - Comparison of target depth and measured final depth achieved for model cable plough centrifuge tests in HST95 sand (at model scale).

Figure 6 - Variation of tow force with depth for different relative densities in dry HST95 sand fitted (a) with Equation 1 proposed by Cathie (2001) showing derived passive pressure coefficient values, C_s, and (b) with Equation 2 proposed by Robinson *et al.* (2017) showing derived values of C_s* (at prototype scale).

Figure 7 - Centrifuge model CPT data (at 50*g*) using a 16 mm diameter cone in (a - c) dry medium dense (D_r = 53 %) HST95 sand and (d - f) dry very dense (D_r = 84 %) HST95 sand (at prototype scale).

Figure 8 - Lateral stress coefficients derived from centrifuge model CPT tests in medium dense (a) and very dense (b) HST95 sand.

Figure 9 - Centrifuge model cable plough data in dry HST95 at different densities fitted with tow forces based on CPT predictions (a) using Equation 4 and (b) using Equation 4 with stress-corrected friction angles (at prototype scale).

Figure 10 - (a) Variation of tow force with plough velocity and (b) normalised final plough depth against plough velocity in very dense saturated HST95 sand for 1/50th scale model cable plough at 50*g* (at prototype scale).

Figure 11 – Variation of rate effect against normalised velocity incorporating the state parameter, ψ, in very dense saturated HST95 sand for 1/50th scale model cable plough at 50*g*, showing the derivation of $C_{dn\psi}$.

Table 1 - Properties of HST95 sand used in the centrifuge tests.

Property	**Value**
Permeability[a] (m/s)	1.23×10^{-4} (17%)
One-dimensional Young's modulus[b] (kN/m^2)	647 (53%)
D_{10} (mm)	0.10
D_{50} (mm)	0.14
Critical state friction angle (degrees)	32
Interface friction angle for aluminium (degrees)	17
Maximum dry density (kg/m^3)	1792
Minimum dry density (kg/m^3)	1487

[a]Permeability and E_0' shown with relative density of sample in parenthesis

[b]E_0' determined at effective stresses relevant to model testing (0.2 - 0.3 kN/m^2)

Table 2 – Summary of centrifuge testing programme using a 1/50th scale model cable plough in HST 95 sand.

Test number	Sand relative density, D_r (%)	Saturation condition	Pore fluid viscosity, η (cP)	Actuator towing speed (m/h)	Scaled plough velocity (m/h)	Model target depth (mm)	Prototype target depth (m)
SR24	86	Dry	-	22	-	50	2.5
SR25	83	Dry	-	22	-	22	1.1
SR26	85	Dry	-	22	-	36	1.8
SR27	43	Dry	-	22	-	36	1.8
SR28	44	Dry	-	22	-	50	2.5
SR29	41	Dry	-	22	-	22	1.1
SR30	81	Saturated	1	99	2	36	1.8
SR31	84	Saturated	1	100	2	50	2.5
SR34	80	Saturated	164	97	318	36	1.8
SR35	82	Saturated	78	96	150	36	1.8

Table 3 – Summary of primary results from the centrifuge testing programme using a 1/50th scale model cable plough in HST 95 sand.

Test number	Measured final depth at model scale (mm)	Model steady state tow force (kN)	Measured final depth at prototype scale (m)	Prototype steady state tow force (kN)	Final plough pitch[a] (°)	Static coefficient, C_s	Modified dimensionless static coefficient, C_s^*	Dimensionless dynamic coefficient incorporating state parameter, $C_{dn\psi}$
SR24	49.7	0.31	2.49	789	-0.3			
SR25	21.0	0.11	1.05	267	-0.3	6.2	3.3	-
SR26	37.1	0.20	1.85	492	-0.4			
SR27	36.9	0.17	1.85	426	-0.3			
SR28	51.0	0.25	2.55	634	-0.4	4.9	2.5	-
SR29	22.0	0.08	1.10	207	-0.3			
SR30	36.0	0.12	1.80	299	-0.2			
SR31	49.0	0.20	2.45	511	0.0	-	-	0.78
SR34	32.5	0.41	1.63	1019	1.6			
SR35	34.5	0.34	1.73	863	0.6			

[a] Positive pitch indicates heel of the plough above the toe, negative indicates heel below the toe.

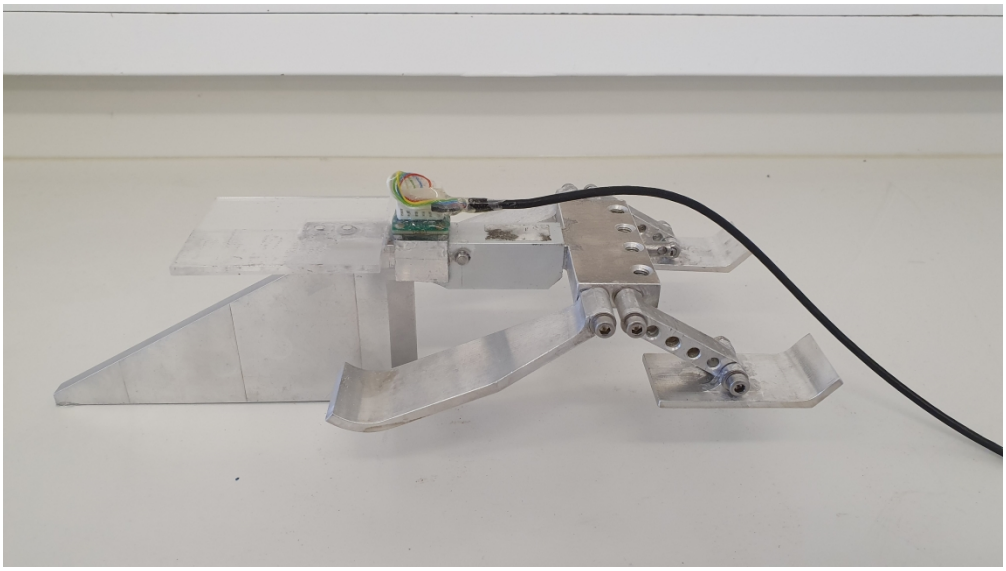

Figure 1 - Image showing the 1/50th scale aluminium model cable plough instrumented with MEMS accelerometer for pitch and roll sensing.

1066x600mm (96 x 96 DPI)

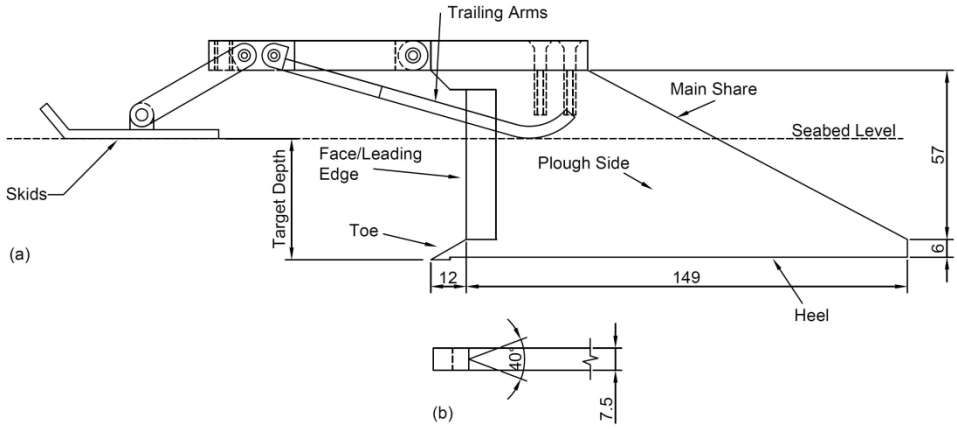

Figure 2 - (a) Side elevation of 1/50th scale model cable plough in ploughing configuration showing key share dimensions, (b) incorporating plan view (in section) of tip geometry (dimensions in mm at model scale).

938x413mm (96 x 96 DPI)

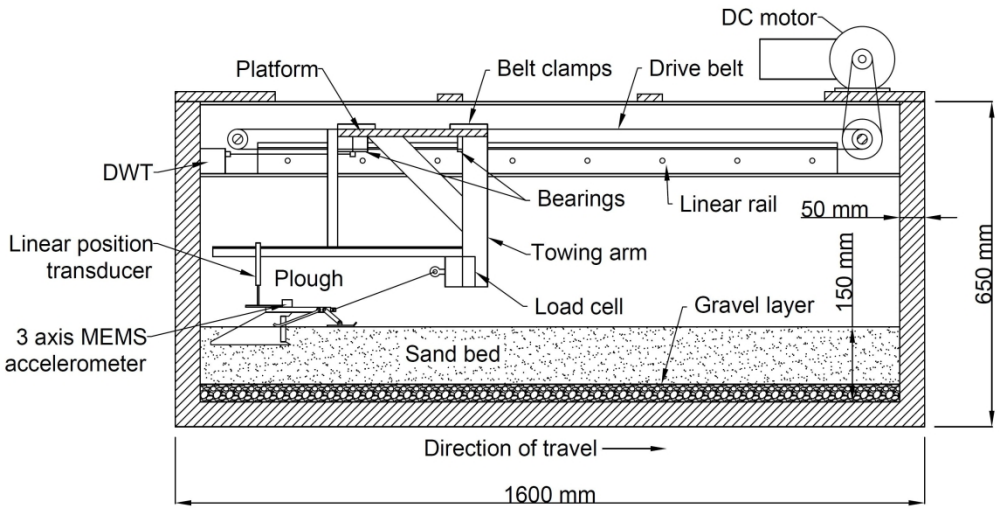

Figure 3 - Schematic showing a cross section of the large displacement centrifuge ploughing actuator and model.

860x495mm (96 x 96 DPI)

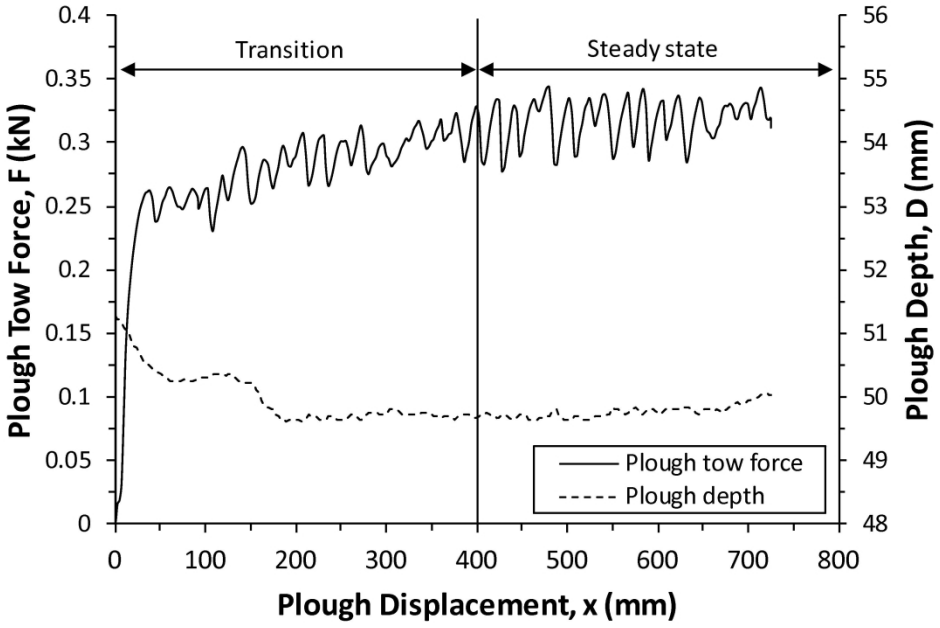

Figure 4 - Variation of pre-embedded model cable plough tow force and depth with displacement from a centrifuge test in very dense dry HST95 sand (D_r = 86 %) with a target depth of 50 mm (at model scale).

150x100mm (600 x 600 DPI)

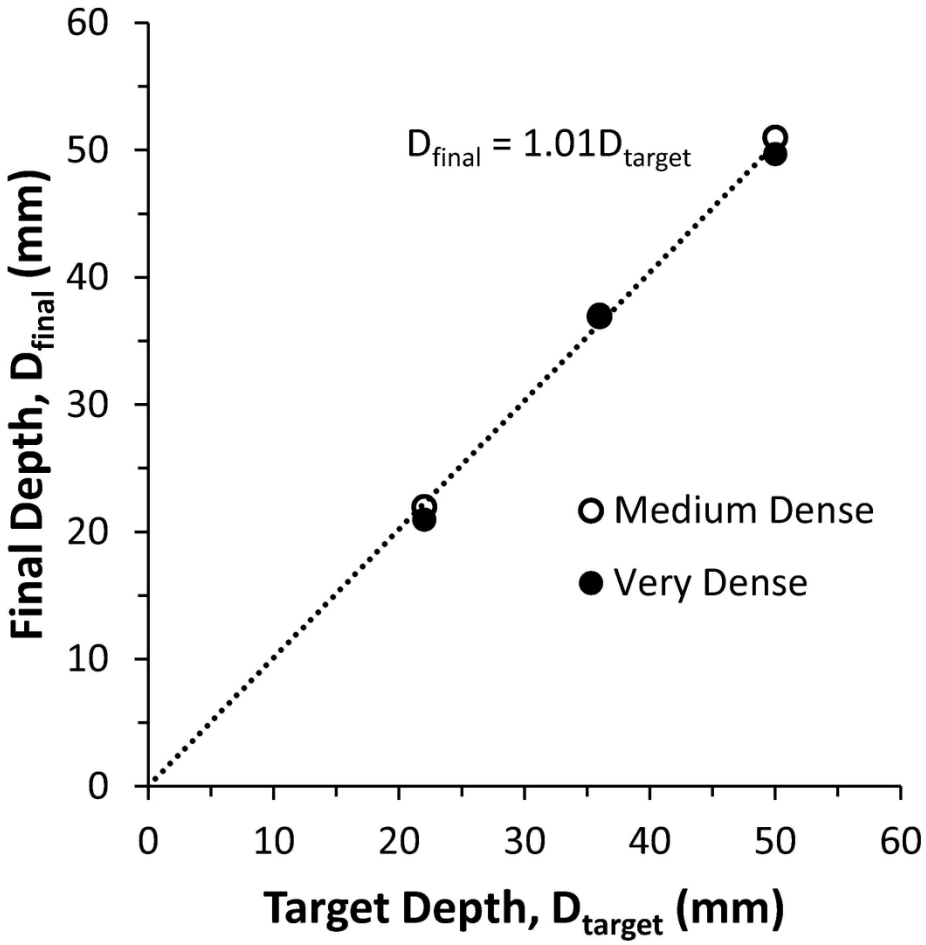

Figure 5 - Comparison of target depth and measured final depth achieved for model cable plough centrifuge tests in HST95 sand (at model scale).

100x100mm (600 x 600 DPI)

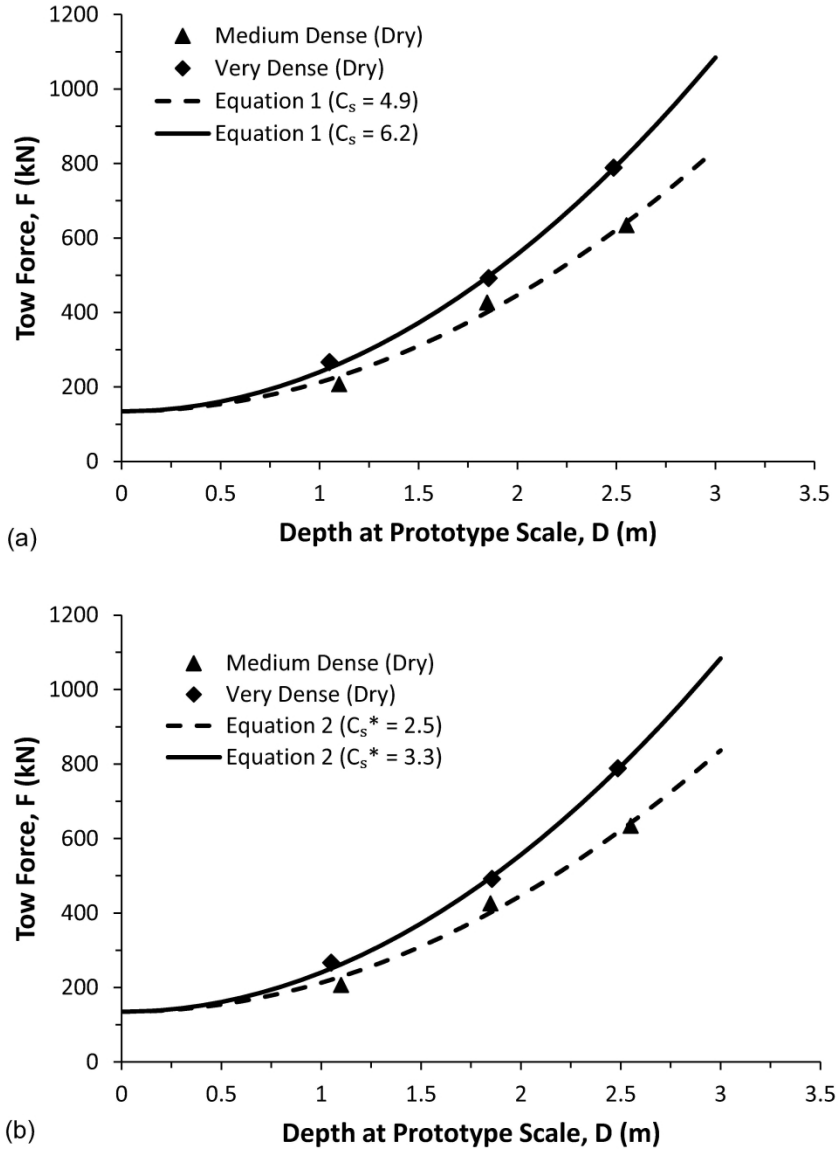

Figure 6 - Variation of tow force with depth for different relative densities in dry HST95 sand fitted (a) with Equation 1 proposed by Cathie (2001) showing derived passive pressure coefficient values, C_s, and (b) with Equation 2 proposed by Robinson et al. (2017) showing derived values of C_s* (at prototype scale).

150x205mm (600 x 600 DPI)

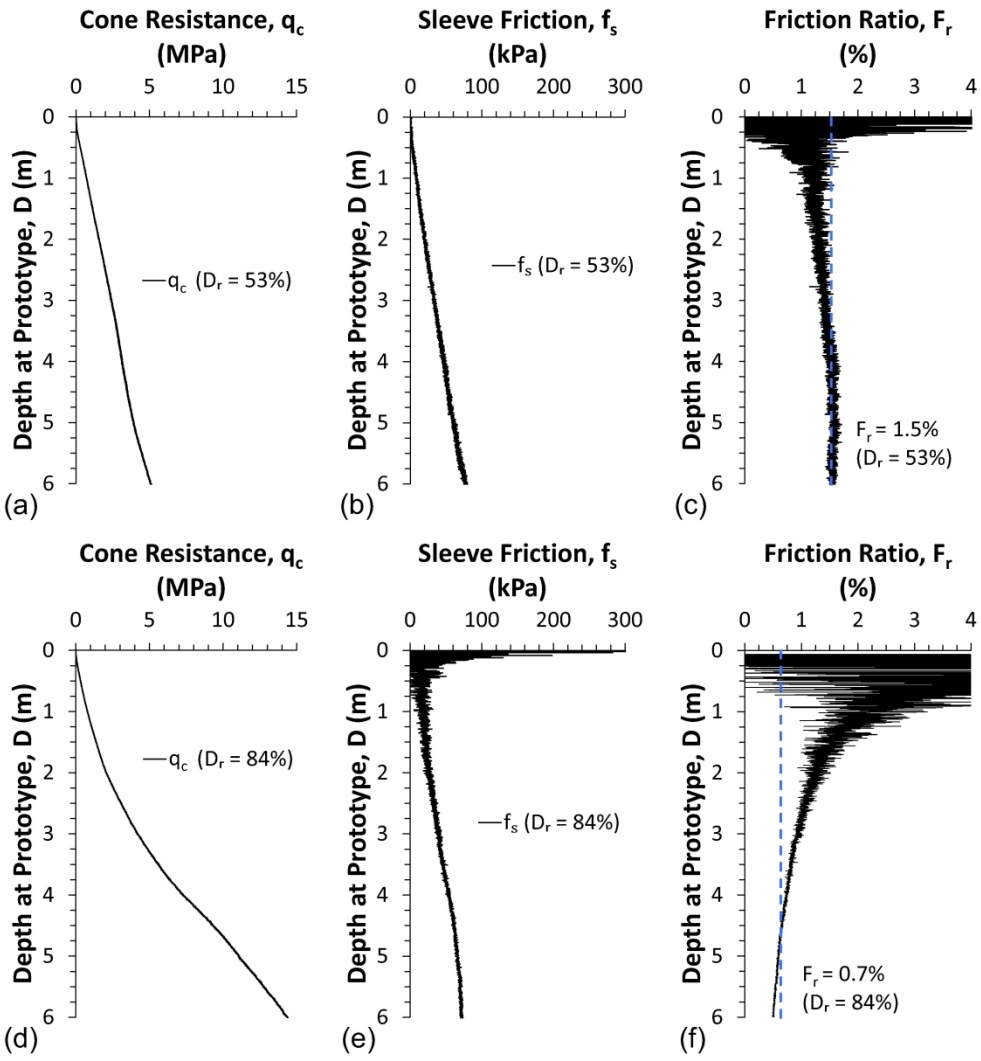

Figure 7 - Centrifuge model CPT data (at 50*g*) using a 16 mm diameter cone in (a - c) dry medium dense (D_r = 53 %) HST95 sand and (d - f) dry very dense (D_r = 84 %) HST95 sand (at prototype scale).

150x159mm (600 x 600 DPI)

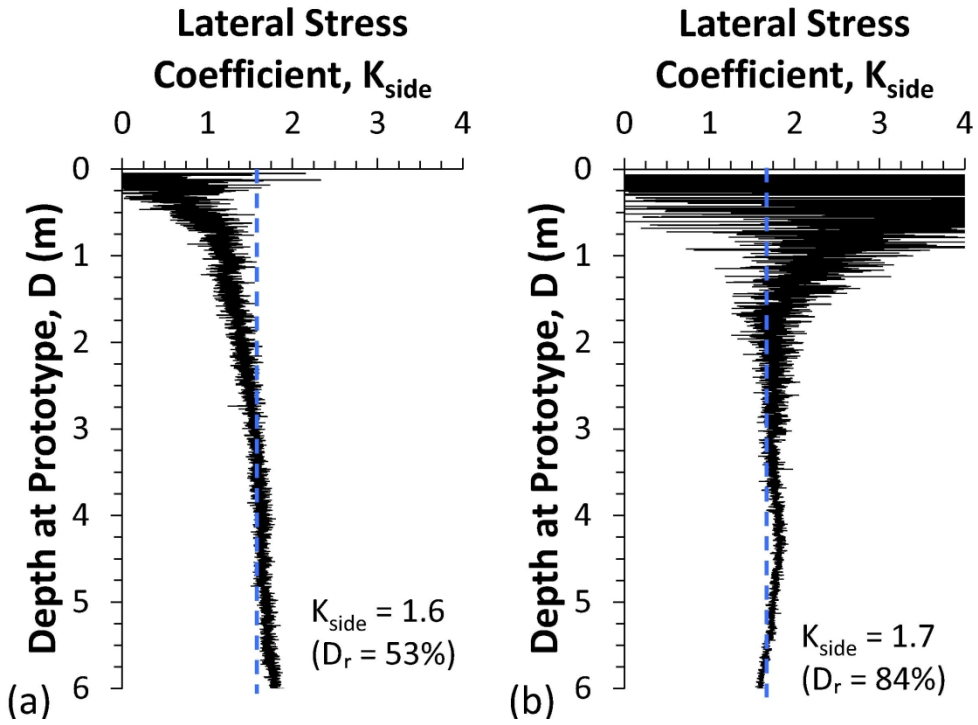

Figure 8 - Lateral stress coefficients derived from centrifuge model CPT tests in medium dense (a) and very dense (b) HST95 sand.

103x77mm (600 x 600 DPI)

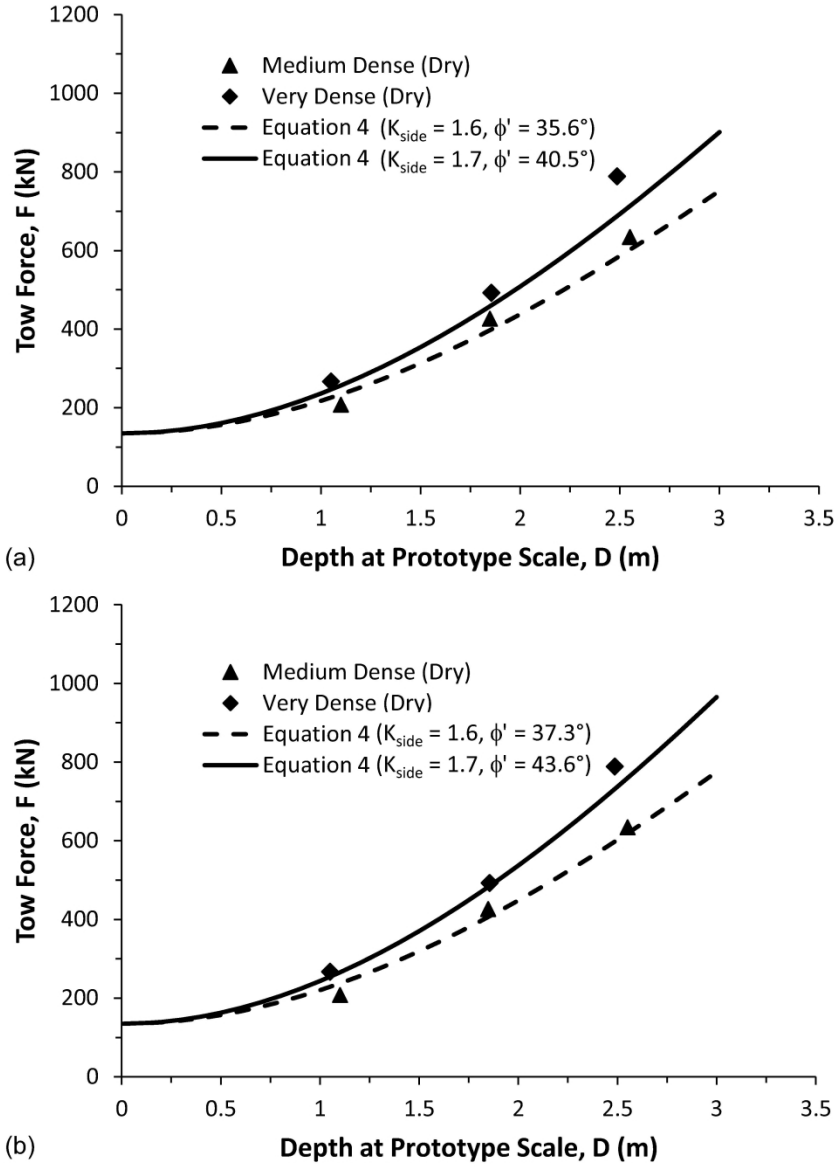

Figure 9 - Centrifuge model cable plough data in dry HST95 at different densities fitted with tow forces based on CPT predictions (a) using Equation 4 and (b) using Equation 4 with stress-corrected friction angles (at prototype scale).

150x205mm (600 x 600 DPI)

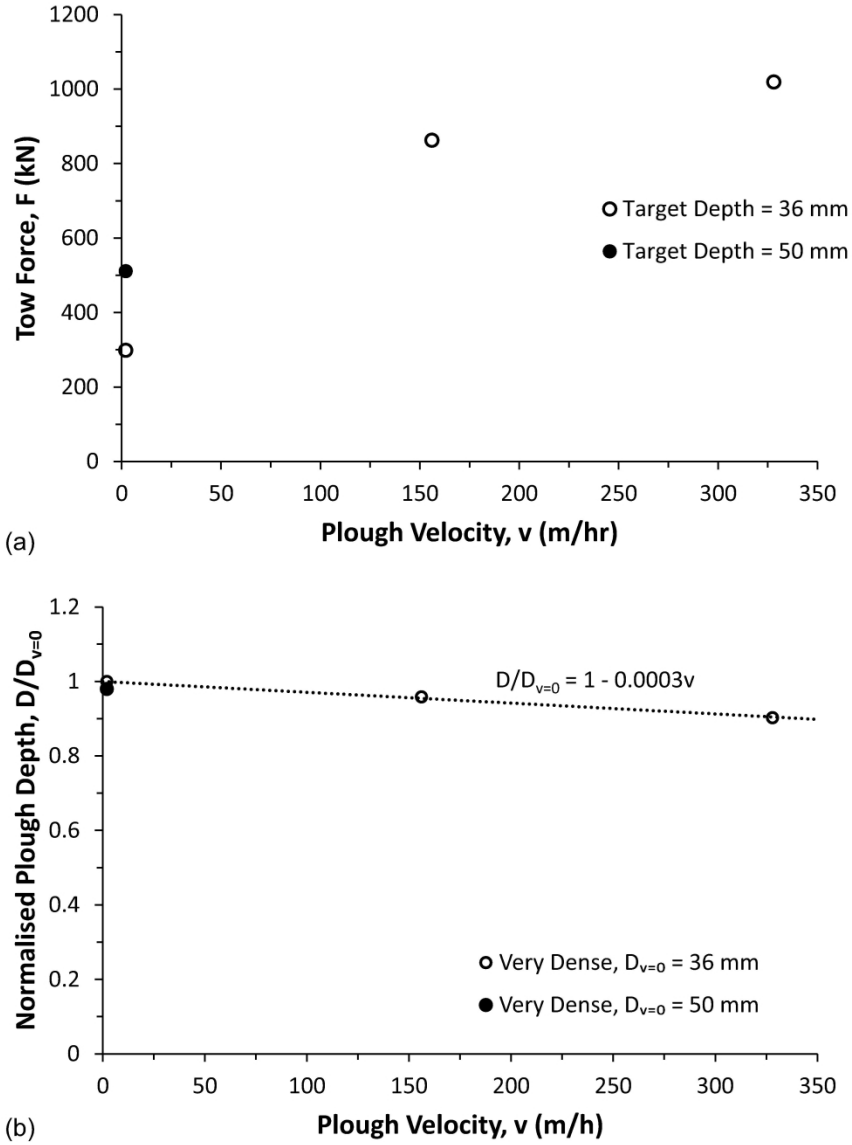

Figure 10 - (a) Variation of tow force with plough velocity and (b) normalised final plough depth against plough velocity in very dense saturated HST95 sand for 1/50th scale model cable plough at 50*g* (at prototype scale).

150x205mm (600 x 600 DPI)

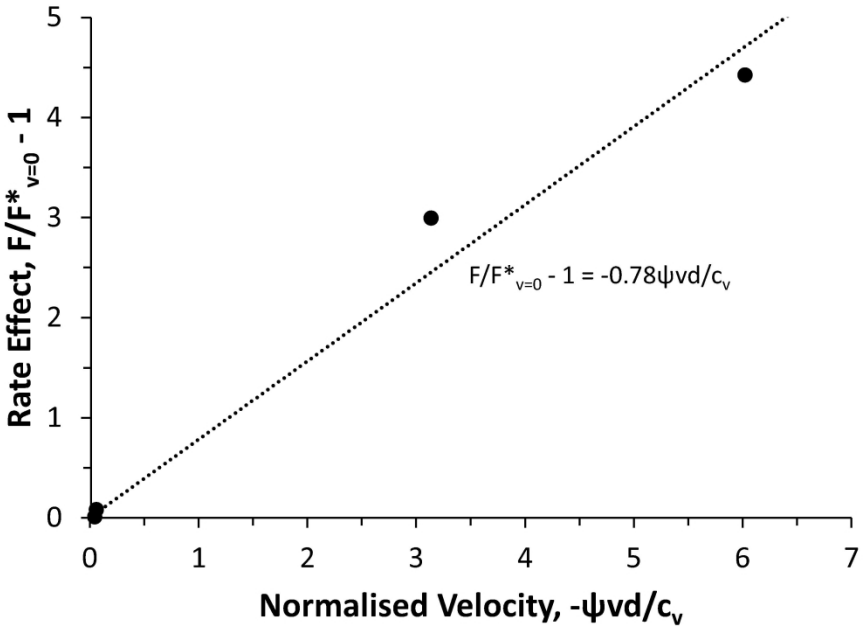

Figure 11 – Variation of rate effect against normalised velocity incorporating the state parameter, ψ, in very dense saturated HST95 sand for 1/50th scale model cable plough at 50g, showing the derivation of $C_{dn\psi}$.

150x100mm (600 x 600 DPI)